# Theoretical Study of Mixed Hydrogen-Bonded Complexes: $H_2O\cdots HCN\cdots H_2O$ and $H_2O\cdots HCN\cdots HCN\cdots H_2O$

**Roberto Rivelino[†] and Sylvio Canuto***

*Instituto de Física, P.O. Box 66318, Universidade de São Paulo, 05315-970 São Paulo, SP, Brazil*

*Received: May 22, 2001; In Final Form: September 25, 2001*

Mixed hydrogen-bonded clusters $H_2O\cdots HCN$, $HCN\cdots H_2O$, $H_2O\cdots HCN\cdots H_2O$, and $H_2O\cdots HCN\cdots HCN\cdots H_2O$ are studied by using ab initio calculations. The optimized structures and harmonic vibrational frequencies are obtained at the DFT/B3LYP and MBPT/MP2 levels with the 6-311++G(d,p) basis set. To investigate electron correlation effects on the binding energies, single-point calculations are also performed using the CCSD(T) method with the optimized MP2 geometries. The complexation energies are obtained for these systems including correction for basis set superposition error. In addition, the cooperative effects in the properties of the complexes are investigated quantitatively. We found a cooperativity contribution of around 10% relative to the total interaction energy of the complex $H_2O\cdots HCN\cdots H_2O$. In the case of $H_2O\cdots HCN\cdots HCN\cdots H_2O$, the binding energy of the $HCN\cdots HCN$ is ca. 8 kJ/mol stronger in the mixed tetramer than in the corresponding isolated dimer. The effects of higher-order electron correlation are found to be mild, with MP2 giving a well-balanced result. Cooperative effects are predicted either by MP2 or by B3LYP in hydrogen bond distances and dipole moments of the clusters. In contrast, the B3LYP functional fails to account for the out-of-plane bend angle in $H_2O\cdots HCN$, which is well-described by the MP2 method.

## 1. Introduction

Experiments on photolysis of formaldoxime in an argon matrix[1] have led to the discovery of different complexes containing hydrogen cyanide and water. Other experimental works on microwave spectroscopy[2,3] have aided characterization of HCN−water complexes. These methods, together with both millimeter-wave and infrared spectra, are also being used to observe a series of other gas-phase molecules existing under special conditions.[4,5] In particular, HCN−water clusters are of great importance in the role of formation of the ancient organic compounds.[6−8] From a theoretical point of view, ab initio calculations carried out with appropriate levels of theory have allowed determination of reliable information about rotational constants, infrared spectra, and structural properties of such complexes.[9−13]

The possible existence of an HCN−water isomer in which the water molecule acts as a proton donor has recently been investigated.[1,9,14] This isomer ($HCN\cdots H_2O$) was experimentally observed and computationally calculated to be less stable than the ordinary hydrogen-bonded mixed dimer ($H_2O\cdots HCN$) by 5.3 kJ/mol[1]. Other theoretical studies have been made by Heikkilä and Lundell[10] for investigating pure dimers of HCN and HNC. Smith et al.,[11] Tshela and Ford,[12] and Turi and Dannenberg[13] performed detailed ab initio calculations on HCN−water mixed dimers. In our previous work,[9] we have analyzed the equilibrium structures and changes in intramolecular vibrational frequencies of the isomers $HCN\cdots H_2O$ and $H_2O\cdots HCN$ with the many-body perturbation (MBPT) and density-functional theories (DFT). To evaluate the electron correlation effects on binding energies of these dimers, we performed single-point calculations employing the coupled-cluster method, carried out with different basis sets.

The formation of a hydrogen-bonded system, involving two species capable of donating and accepting a proton simultaneously, provides a complex that is both a stronger proton donor and a stronger proton acceptor. This effect is currently attributed to an electron density transfer from the acceptor to the donor across the hydrogen bonding, which can extend itself for a long range of intermolecular interaction, forming chains or cycles, and it is usually known as cooperativity.[15,16] Experimentally, the cooperative effect can be observed in several hydrogen-bonded systems, including liquids and crystal structures.[17,18] Theoretically, such interactions have been described as $\sigma$-bond cooperativity, in contrast to those with multiple bonds, which are known as $\pi$-bond cooperativity.[19] It is common in the literature to employ the term nonadditivity to express the cooperativity quantitatively, as the total interaction energy of a hydrogen-bonded complex on one hand and the sum of all pairwise interactions on the other.[20] Further evidence of the cooperative effects arises from consideration of the geometry, dipole moment, and vibration frequencies of hydrogen-bonded clusters. Theoretical studies taking into account of these effects have become an important subject to understand the nature of interactions in many-molecule clusters as they occur in biological, chemical, and physical systems.[21−23]

This paper is an extension of our previous study on HCN−water complexes to other theoretically predicted linear clusters, namely, the mixed trimer $H_2O\cdots HCN\cdots H_2O$ and the mixed tetramer $H_2O\cdots HCN\cdots HCN\cdots H_2O$. This tetramer is a possible product of the interaction between the two isomers $H_2O\cdots HCN$ and $HCN\cdots H_2O$. Thus, we have made a detailed analysis of the structures, harmonic vibrational frequencies, energetics, and effects of cooperativity on the properties of these complexes. The ab initio calculations used here are the DFT and MBPT/coupled-cluster theories successfully used to investigate HCN−water isomers.[9]

* To whom correspondence should be addressed. E-mail: canuto@if.usp.br. Fax: +55.11.3818-6831.
[†] E-mail: rivelino@if.usp.br.

10.1021/jp011966f CCC: $20.00 
Published on Web 11/22/2001

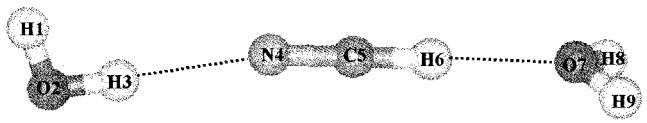


$H_2O\cdots HCN\cdots H_2O$

**Figure 1.** Structure of the trimer $H_2O\cdots HCN\cdots H_2O$.

## 2. Computational Aspects

Quantum chemistry computations have been applied to the systems $H_2O\cdots HCN$, $HCN\cdots H_2O$, $H_2O\cdots HCN\cdots H_2O$, and $H_2O\cdots HCN\cdots HCN\cdots H_2O$ using the Gaussian 98 program.[24] These are the density functional theory with gradient-corrected exchange-correlation (DFT/B3LYP)[25,26] and the second-order many-body perturbation theory (MBPT/MP2), both carried out with the 6-311++G(d,p) basis set to full optimization of the geometries. After the equilibrium structures are found, at the MP2 and B3LYP levels of theory, we have calculated their vibrational spectra. This guarantees that each optimized structure corresponds to an energy minimum. The MP2 energies have been improved for electron correlation effects by performing single-point calculations with many-body perturbation/coupled cluster methods carried out with the same basis set. These include MP3, MP4, CCSD, and CCSD(T)[27,28] calculations.

The interaction energies of the clusters have been corrected for basis set superposition error (BSSE) using the counterpoise correction method (CP).[29,30] The cooperative energy component of $H_2O\cdots HCN\cdots H_2O$ is defined in the usual manner,[20] by considering two reaction routes for obtaining the trimer. The three-body term is computed as the difference between the binding energy of the trimer and the pairwise interaction energies:

$$E_{ABC} = \Delta E - [\Delta E(AB) + \Delta E(AC) + \Delta E(BC)]$$

To evaluate the energetics of the mixed tetramer $H_2O\cdots HCN\cdots HCN\cdots H_2O$, we have used a two-body approximation in such a way that the basic moieties are considered as being the dimers $H_2O\cdots HCN$ and $HCN\cdots H_2O$. In this case, the binding energy is computed as the total energy of the tetramer minus the energy sum of the separate dimers. Corrections for zero-point vibration energy are also calculated from the harmonic frequency analysis.

## 3. Results and Discussion

**Geometrical Features of the Mixed Trimer.** The optimized geometry of $H_2O\cdots HCN\cdots H_2O$ is illustrated in Figure 1, and its geometrical parameters are presented in Table 1 at the two levels of calculation (MP2 and B3LYP). The main difference between the results of these methods is the out-of-plane bend angle, $\delta$, that the water molecule forms when it acts as a proton acceptor in the complex. Our calculated MP2 value for $\delta$ in $H_2O\cdots HCN\cdots H_2O$ is 24°, whereas the B3LYP value is only 7.8°.

As we shall see later, the out-of-plane bend angle calculated in $H_2O\cdots HCN$ at the MP2 level is 23° (see Table 3). This value is in good agreement with the rotational spectroscopy experiments, which furnish 20°.[3] For this reason, we believe that in the case of the trimer the MP2 calculations provide more reliable potential surfaces than the B3LYP ones. Another interesting feature observed in the geometry of $H_2O\cdots HCN\cdots H_2O$ is that the intermolecular distances (O···H and N···H) are shorter at the B3LYP level than those obtained from MP2 calculations. The cooperativity in the hydrogen bond distances appears when we compare the O7···H6 distance in the trimer with the corresponding one in the dimer $H_2O\cdots HCN$. The latter distance has been computed as 2.067 Å (at the MP2 level), showing that when a second $H_2O$ molecule is added as a proton donor, it contracts the O7···H6 distance by about 0.04 Å.

**TABLE 1: Geometry of $H_2O\cdots HCN\cdots H_2O$ Complex Computed with Different Methods[a]**

| geometry | MP2/6-311++G(d,p) | B3LYP/6-311++G(d,p) |
|---|---|---|
| O2−H1 | 0.959 | 0.961 |
| O2−H3 | 0.964 | 0.968 |
| N4···H3 | 2.128 | 2.098 |
| C5−N4 | 1.170 | 1.149 |
| C5−H6 | 1.077 | 1.079 |
| O7···H6 | 2.031 | 1.987 |
| O7−H8 | 0.961 | 0.963 |
| O7−H9 | 0.961 | 0.963 |
| H1−O2−H3 | 103.0 | 104.6 |
| H8−O7−H9 | 104.2 | 106.0 |
| $\delta$ (deg) | 24.0 | 7.8 |
| $\mu$ (D) | 7.86 | 7.93 |
| $I_A$ (GHz) | 150.405 | 200.700 |
| $I_B$ (GHz) | 1.007 | 1.026 |
| $I_C$ (GHz) | 1.005 | 1.026 |

[a] Distances are given in Å, and angles are given in deg. The out-of-plane angle, $\delta$, dipole moment, $\mu$, and rotational constants ($I_A$, $I_B$, $I_C$) are also shown.

Table 1 also gives the dipole moments of $H_2O\cdots HCN\cdots H_2O$. The dipole moment of the complex is slightly larger than the dipole sum of the three individual monomers. For example, at the MP2 level, the sum is 7.84 D, compared to the calculated value of 7.86 D for the trimer. At the B3LYP level, this increase becomes more meaningful, from 7.37 to 7.93 D, respectively. This dipole increment can be understood by cooperative polarization effect when the hydrogen-bonded chain grows. Rotational constants are also shown in Table 1. Because the trimer has not been observed experimentally, a direct comparison with observed rotational constants cannot be made. Judging from our previous result on the $H_2O\cdots HCN$ isomer,[9] we believe that the $I_B$ and $I_C$ constants are accurate within 1% or less.

**Complexation Energies of $H_2O\cdots HCN\cdots H_2O$.** The components of the complexation energy of the mixed trimer are reported in Table 2. Comparison with the SCF results allows separation of the contribution of the electron correlation effects. All results were corrected for BSSE using the counterpoise method. They are organized in two different paths for obtaining the trimer, $H_2O\cdots HCN\cdots H_2O$. First, we combine a $H_2O$ molecule with HCN forming the most stable dimer, $H_2O\cdots HCN$, which we call dimer I. This is added to another $H_2O$ molecule acting as a proton donor (Path I). The same complex is obtained in Path II, in which one combines HCN plus $H_2O$, forming the less stable dimer, $HCN\cdots H_2O$ or dimer II, and then adds the second $H_2O$ molecule as a proton acceptor. The two procedures are given in the following scheme:

**Path I**

$$\text{I-A:}\quad H_2O + HCN \rightarrow H_2O\cdots HCN$$

$$\text{I-B:}\quad H_2O\cdots HCN + H_2O \rightarrow H_2O\cdots HCN\cdots H_2O$$

**Path II**

$$\text{II-A:}\quad HCN + H_2O \rightarrow HCN\cdots H_2O$$

$$\text{II-B:}\quad H_2O + HCN\cdots H_2O \rightarrow H_2O\cdots HCN\cdots H_2O$$

The total energy of the trimer is, of course, the same, regardless of the path chosen. Comparison of reactions I-B and II-A at

**TABLE 2: Complexation Energies (in kJ/mol) and Cooperative Effect in $H_2O\cdots HCN\cdots H_2O$ Complex Computed with the 6-311++G(d,p) Basis Set[a]**

| energy | SCF | MP2 | MP3 | DQ-MP4 | SDQ-MP4 | MP4 | CCSD | CCSD(T) | B3LYP |
|---|---|---|---|---|---|---|---|---|---|
| *E*(I-A) | −21.17 | −19.48 | −19.73 | −19.05 | −18.93 | −18.84 | −18.84 | −18.93 | −21.80 |
| *E*(I-B) | −15.32 | −17.98 | −16.69 | −16.58 | −16.79 | −17.36 | −16.61 | −17.11 | −21.61 |
| *E*(II-A) | −11.70 | −14.59 | −13.27 | −13.19 | −13.39 | −13.97 | −13.21 | −13.71 | −14.61 |
| *E*(II-B) | −24.79 | −22.86 | −23.16 | −22.44 | −22.33 | −22.23 | −22.25 | −22.33 | −28.80 |
| total[b] | −36.49 | −37.45 | −36.42 | −35.63 | −35.71 | −36.20 | −35.45 | −36.04 | −43.41 |
| cooperative[c] | −3.62 | −3.39 | −3.42 | −3.39 | −3.40 | −3.39 | −3.40 | −3.41 | −6.99 |
| three-body[d] | −2.42 | −2.27 | −2.32 | −2.29 | −2.31 | −2.31 | −2.31 | −2.32 | −5.91 |

[a] All results are corrected for BSSE. [b] $E$(I-A + I-B) = $E$(II-A + II-B). [c] $E$(I-B − II-A) = $E$(II-B − I-A). [d] $E_{ABC} = E(ABC) - [E(AB) + E(AC) + E(BC)] + [E(A) + E(B) + E(C)]$.

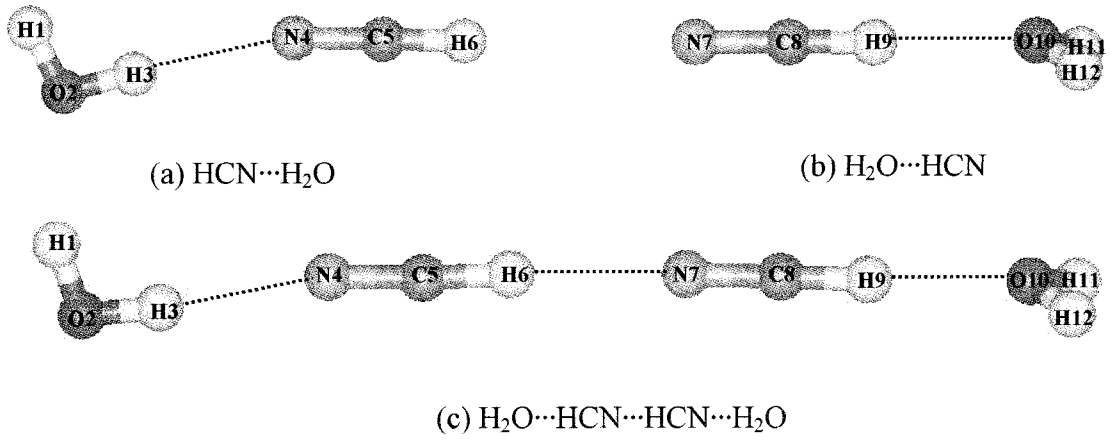


**Figure 2.** Calculated structures of the HCN−water complexes: (a) the less stable dimer II; (b) the more stable dimer I; (c) the tetramer.

the MP2 level shows that $H_2O$, acting as a proton donor, bonds more strongly to the dimer I (17.98 kJ/mol) than to the isolated HCN molecule (14.59 kJ/mol), as indicated by the energy differences in Table 2. A similar comparison between reactions I-A and II-B shows that the $H_2O$ molecule is a better proton acceptor when it is added first to the dimer II (22.86 kJ/mol) than to a single HCN molecule (19.48 kJ/mol). The energy enhancement in the trimer formation is better described by the cooperative energy (Table 2) of 3.4 kJ/mol, calculated with the MP2 method (and about twice that amount for the B3LYP level).

It is interesting to note that in this case the cooperative effects are not very much dependent on the electron correlation contribution beyond MP2. For instance, one can note that the binding energy changes from 35.7 kJ/mol to 36.2 kJ/mol by including triple excitation in fourth-order. However, the contribution to the cooperative effects is only 0.01 kJ/mol. Similarly, the cooperativity contribution using CCSD or CCSD(T) is the same. By far, most of the cooperativity is obtained already in MP2. On the other hand, the DFT/B3LYP model seems to overestimate significantly these quantities, giving results that are more than twice those obtained at the CCSD(T) level.

The cooperative energy terms calculated in Table 2 take into account the contributions arising from the interaction between the two terminal water molecules. Thus, we have also computed the three-body term by defining it as the total binding energy of the trimer minus the interaction energy of each pair of monomers with all of them frozen in the geometry of the trimer.[20] As it can be seen, the three-body contribution is small, being less than 2.5 kJ/mol, in all theoretical models considered here, except to the B3LYP level. This corresponds to only ∼6% of the total complexation energy. Again, electron correlation effects seem to be less important for the three-body terms reported in Table 2. As noted before by Chalasinski and Szczesniak,[31] these energy components are reasonably well-described at the SCF level. In fact, the cooperative energy is computed as being −3.62 kJ/mol (and −2.42 kJ/mol for the three-body term) with SCF calculation, while at the highest level, CCSD(T), these terms are −3.41 kJ/mol (and −2.32 kJ/mol). This behavior holds for any level of higher-order electron correlation calculated in the MBPT/coupled-cluster series (Table 2).

**Dimer and Tetramer Geometries.** The structures of the mixed dimers, $H_2O\cdots HCN$ and $HCN\cdots H_2O$, and the tetramer, $H_2O\cdots HCN\cdots HCN\cdots H_2O$, are shown in Figure 2. The geometries of these systems are also fully optimized at the MP2/6-311++G(d,p) and B3LYP/6-311++G(d,p) levels. The geometrical parameters for their equilibrium structures are presented in Table 3. We observe that the O10···H9 bonding is shorter in the resultant tetramer by 0.05 Å at the MP2 level and 0.06 Å at the B3LYP level relative to the dimer I. A similar result is also obtained when $H_2O$ acts as a proton donor. For this case, an enhancement in the calculated N4···H3 distance (0.03 Å with MP2 and 0.05 Å with B3LYP) can still be seen. A more significant decrease is observed in the N7···H6 bonding; it is 0.1 Å with respect to the corresponding bonding in the HCN···HCN dimer (calculated as 2.271 Å at the MP2 level).

These effects of cooperativity are less apparent in the intramolecular geometry (Table 3). For instance, the H−O−H angle remains essentially constant when the complex increases. On the other hand, the intermolecular O2−H3−N4 angle is slightly more sensitive; it varies 3.5° from the dimer II to the tetramer with either MP2 or B3LYP. Conversely, as we have discussed previously, the $\delta$ bend angle (which indicates how the proton acceptor $H_2O$ molecule is out-of-plane in the complex) is better described with the MP2 method. For this level of theory, our calculated $\delta$ is 23° in the dimer I and 21° in the tetramer (Table 3). The values obtained with the B3LYP calculations are only 3.2° and 0.5°, respectively. Indeed, experimental results for the dimer I give an angle of 20°.[3] It is also interesting to observe here a cooperative polarization effect

**TABLE 3: Optimized Geometries of the HCN−Water Dimers and Tetramer[a]**

| | MP2/6-311++G(d,p) | | | B3LYP/6-311++G(d,p) | | |
|---|---|---|---|---|---|---|
| geometry | dimer I | dimer II | tetramer | dimer I | dimer II | tetramer |
| O2−H1 | | 0.959 | 0.959 | | 0.961 | 0.961 |
| O2−H3 | | 0.963 | 0.965 | | 0.967 | 0.968 |
| N4···H3 | | 2.167 | 2.140 | | 2.140 | 2.093 |
| C5−N4 | | 1.170 | 1.170 | | 1.480 | 1.149 |
| C5−H6 | | 1.068 | 1.077 | | 1.067 | 1.078 |
| N7···H6 | | | 2.173 | | | 2.129 |
| C8−N7 | 1.172 | | 1.170 | 1.150 | | 1.149 |
| C8−H9 | 1.076 | | 1.078 | 1.077 | | 1.080 |
| O10···H9 | 2.067 | | 2.015 | 2.028 | | 1.969 |
| O10−H11 | 0.961 | | 0.961 | 0.963 | | 0.963 |
| O10−H12 | 0.961 | | 0.961 | 0.963 | | 0.963 |
| H1−O2−H3 | | 103.2 | 102.9 | | 104.8 | 104.6 |
| O2−H3−N4 | | 179.1 | 175.5 | | 178.5 | 175.1 |
| H11−O10−H12 | 104.1 | | 104.2 | 105.9 | | 106.2 |
| $\delta$ (deg) | 23.0 | | 21.0 | 3.2 | | 0.5 |
| $\mu$ (D) | 6.06 | 5.36 | 12.34 | 5.85 | 5.11 | 12.17 |
| $I_A$ (GHz) | 401.031 | 481.461 | 124.641 | 423.923 | 524.624 | 181.396 |
| $I_B$ (GHz) | 3.046 | 3.176 | 0.329 | 3.121 | 3.235 | 0.337 |
| $I_C$ (GHz) | 3.027 | 3.155 | 0.329 | 3.099 | 3.215 | 0.337 |

[a]Distances are given in Å and angles are given in deg. The out-of-plane angle, $\delta$, dipole moment, $\mu$, and rotational constants ($I_A$, $I_B$, $I_C$) are also shown.

**TABLE 4: Influence of Electron Correlation and Counterpoise Correction on the Binding Energies (in kJ/mol) of the Mixed Tetramer Relative to the Separate Dimers I and II and $(HCN)_2$[a]**

| | no counterpoise correction | | | | counterpoise correction | | | |
|---|---|---|---|---|---|---|---|---|
| method | tetramer | dimer I | $(HCN)_2$ | dimer II | tetramer | dimer I | $(HCN)_2$ | dimer II |
| SCF | 27.82 | 23.13 | 18.90 | 13.50 | 26.84 | 21.41 | 17.67 | 12.04 |
| MP2 | 28.58 | 25.25 | 19.49 | 16.97 | 26.08 | 19.67 | 17.72 | 14.80 |
| MP3 | 27.66 | 24.97 | 18.83 | 16.05 | 25.13 | 19.94 | 16.73 | 13.50 |
| DQ-MP4 | 27.56 | 24.34 | 18.84 | 15.84 | 25.09 | 19.30 | 16.84 | 13.46 |
| SDQ-MP4 | 27.77 | 24.51 | 18.91 | 16.05 | 25.25 | 19.18 | 16.94 | 13.63 |
| MP4 | 28.22 | 25.15 | 19.16 | 16.68 | 25.46 | 19.07 | 17.15 | 14.17 |
| CCSD | 27.39 | 24.32 | 18.63 | 15.93 | 24.89 | 19.10 | 16.62 | 13.46 |
| CCSD(T) | 27.82 | 24.98 | 18.89 | 16.47 | 25.12 | 19.16 | 16.81 | 13.96 |
| B3LYP | 28.54 | 24.45 | 19.99 | 15.84 | 27.73 | 22.27 | 17.96 | 15.13 |

[a] Values were computed with the 6-311++G(d,p) basis set. Differences in zero-point vibration energy in the tetramer are 3.75 and 4.77 kJ/mol for the calculated frequencies with the MP2 and B3LYP methods, respectively.

on the dipole moment of $H_2O\cdots HCN\cdots HCN\cdots H_2O$. The additive MP2 dipole moment of the two HCN−water dimers gives 11.42 D, while the dipole moment of the tetramer is 12.34 D (these are 10.96 and 12.17 D, respectively, with the B3LYP functional). This formation of the tetramer leads to an increase of about 10% in the combined dipole moment.

**$H_2O\cdots HCN\cdots HCN\cdots H_2O$.** The full treatment of the interaction energy of $H_2O\cdots HCN\cdots H_2O$ has shown that the three-body contribution to its total binding energy amounts to only 6%. In previous investigations, it has also been noted that four-body contribution is negligible in the water tetramer[15] and is only ∼10% of the three-body contribution.[16,20] Although the partitioning of the energy in the many-body components is an important issue, our major interest lies in the cooperative effects in the HCN···HCN binding. Here, we are interested in obtaining the interaction energy between the two mixed dimers, $HCN\cdots H_2O$ (Figure 2a) and $H_2O\cdots HCN$ (Figure 2b), leading to the formation of $H_2O\cdots HCN\cdots HCN\cdots H_2O$ and then making a direct comparison with the simpler HCN···HCN, as well as the isolated dimers I and II. Thus, the energetics to form the tetramer (in the fully optimized MP2 and B3LYP geometries) are reported in Table 4 and compared with $(HCN)_2$.

We can see that the B3LYP method gives the largest binding energy for the tetramer, 27.73 kJ/mol, whereas the MP2 result is 26.08 kJ/mol after counterpoise correction. This result reinforces the trend that DFT overestimates binding energies.[32] Our values for the binding energies increase when various hydrogen bonds are involved in the cluster formation. For comparison, the calculated binding energy of the HCN···HCN dimer is 17.72 kJ/mol at the MP2 level with counterpoise correction. This result reflects the electron charge redistribution in the electronic structure of each subunit making the dimer I a stronger proton acceptor and the dimer II a better proton donor when they interact to form the tetramer. Here, the correlation effects investigated with the MBPT/coupled-cluster methods also seem to be not very important. After counterpoise correction, the result obtained with CCSD(T) differs from SCF by less than 2 kJ/mol. In any case, the effect of electron correlation decreases the calculated binding energy. We observe that the contribution of triple excitation at higher order, as obtained from the difference between MP4 and CCSD(T), is only 0.34 kJ/mol. On the other hand, the basis set superposition error gives a larger variation on the binding energies. The counterpoise correction with the MBPT methods is 2.5 kJ/mol, although with the B3LYP functional this effect is only 0.8 kJ/mol. Considering the correction due to zero-point vibration (3.75 kJ/mol at MP2 level), we estimate a binding energy of 22.3 kJ/mol with respect to dissociation of the tetramer into two dimers, $H_2O\cdots HCN$ and $HCN\cdots H_2O$, after breaking the HCN···HCN bond. This illustrates the large cooperative effect derived from the water molecules because this value is more than 8 kJ/mol higher than in the isolated HCN···HCN dimer dissociation (for which the calculated zero-point vibration energy is 3.43 kJ/mol at the MP2 level). Indeed, this cooperative effect is large and essentially

**TABLE 5: Computed Frequencies (in cm$^{-1}$) of Intramolecular Vibrational Modes in the Trimer Compared to HCN and $H_2O$ Molecules[a]**

| | basic moieties[b] | | | $H_2O\cdots HCN\cdots H_2O$ | |
|---|---|---|---|---|---|
| normal modes[c] | MP2 | B3LYP | expt[d] | MP2 | B3LYP |
| HCN stretching ($\pi$) | 729 | 767 | 712 | 888 | 897 |
| HCN bending ($\pi$) | 729 | 767 | 712 | 924 | 930 |
| $H_2O$ scissor ($a_1$) | 1628 | 1602 | 1590 | 1664 (1661) | 1628 (1633) |
| HCN stretching ($\sigma$) | 2016 | 2197 | 2097 | 2029 | 2192 |
| HCN asym stretch ($\sigma$) | 3482 | 3452 | 3311 | 3356 | 3297 |
| $H_2O$ stretching ($a_1$) | 3884 | 3817 | 3638 | 3835 (3872) | 3746 (3817) |
| $H_2O$ asym stretch ($b_2$) | 4003 | 3923 | 3733 | 3975 (3983) | 3894 (3918) |

[a] Data were obtained with the 6-311++G(d,p) basis set. [b] Refer to the $H_2O$ and HCN molecules. [c] Relative to the isolated moieties. [d] References 33 and 34.

**TABLE 6: Frequency (in cm$^{-1}$) Shifts in the Tetramer Relative to the Dimers[a]**

| | $H_2O\cdots HCN$ | | $HCN\cdots H_2O$ | | $H_2O\cdots HCN\cdots HCN\cdots H_2O$ | | | |
|---|---|---|---|---|---|---|---|---|
| normal modes[b] | MP2 | B3LYP | MP2 | B3LYP | MP2 | | B3LYP | |
| $\nu(\pi)$ bending | 877 | 880 | 736 | 774 | 890 | 869 | 908 | 894 |
| $\nu(\pi)$ bending | 908 | 909 | 738 | 775 | 929 | 873 | 941 | 896 |
| $\nu(a_1)$ scissor | 1642 | 1627 | 1654 | 1625 | 1665 | 1645 | 1636 | 1629 |
| $\nu(\sigma)$ sym stretch | 2015 | 2182 | 2031 | 2209 | 2043 | 2030 | 2195 | 2189 |
| $\nu(\sigma)$ asym stretch | 3375 | 3321 | 3481 | 3452 | 3349 | 3334 | 3308 | 3279 |
| $\nu(a_1)$ sym stretch | 3874 | 3818 | 3851 | 3769 | 3872 | 3832 | 3814 | 3743 |
| $\nu(b_2)$ asym stretch | 3989 | 3921 | 3979 | 3898 | 3987 | 3974 | 3917 | 3893 |

[a] Data were computed with the 6-311++G(d,p) basis set. [b] Relative to $H_2O$ and HCN vibrational modes.

independent of the electron correlation effects. For instance, it amounts to 8.36 (MP2), 8.31 (MP4), and 8.31 kJ/mol (CCSD(T)) in different treatments. At the SCF level, it gives an overestimated value of 9.17 kJ/mol. The B3LYP results are closer to the SCF than the MBPT/CC values, giving a cooperative effect of 9.77 kJ/mol. For comparison, we also report in Table 4 the binding energy calculated at MBPT/coupled-cluster level for the dimers I and II. Our best result of 16.8 kJ/mol for $(HCN)_2$ agrees very well with the one of Heikkilä and Lundell[10] (also 16.8 kJ/mol) using a larger basis set 6-311++G(2d,2p).

**Vibrational Analysis of the Complexes.** The frequency shift in infrared spectroscopy is a very useful tool for the characterization of hydrogen-bonded clusters. In the systems studied here, water acts as both acceptor and donor of proton. When it is a proton donor, there appears a large negative shift of the O−H stretching vibrations. In both trimer and tetramer, $H_2O$ acts as a proton donor at one end and a proton acceptor at the other. The calculated vibrational modes for these complexes are given in Tables 5 and 6, respectively. Table 5 shows that the degenerate $\pi$ mode of HCN splits in the trimer, but both undergo a large positive shift. The $\sigma$ stretching vibrations change a little for the symmetric case but undergo a large red shift in the case of the asymmetric stretching. The magnitude of this shift is −126 (MP2) and −155 cm$^{-1}$ (B3LYP).

The changes in the water spectrum are now interesting because of the vibration split of the separate molecules. The bending (scissor) mode of $H_2O$ shows a small splitting of 3 (MP2) and 5 cm$^{-1}$ (B3LYP), which are blue-shifted compared to the individual vibrations. These shifts are +36 (MP2) and +26 cm$^{-1}$ (B3LYP) when $H_2O$ acts as a proton donor and +32 (MP2) and 31 cm$^{-1}$ (B3LYP) when it acts as a proton acceptor. More pronounced splitting is found for the stretching vibration of water. In this case (at the MP2 level), the symmetric stretching of $H_2O$ splits by +37 cm$^{-1}$ corresponding to shifts of −49 and −12 cm$^{-1}$ of the individual molecules. The respective B3LYP calculated shifts are larger, except when water is a proton acceptor, for which no shift is calculated. A very similar behavior is also obtained for the asymmetric vibrational mode at the two levels of theory.

In Table 6, the calculated frequencies are shown for the tetramer in comparison with those of the two HCN−water dimers. Each vibrational frequency is split because of the presence of these dimers in the complex. For this reason, we analyzed the vibrational changes based on the average frequencies for the dimers I and II and the average frequency splitting in the tetramer spectrum. At the MP2 level of calculation, the average symmetric and asymmetric stretching modes of $H_2O$ are −11 and −4 cm$^{-1}$, respectively, whereas for the scissor mode, the value is +7 cm$^{-1}$. All of the average bending vibrational frequencies are positively shifted by 73 and 78 cm$^{-1}$. The average symmetric stretching of HCN is also blue-shifted by 14 cm$^{-1}$. However, the asymmetric mode is considerably red-shifted by 87 cm$^{-1}$.

At the B3LYP level, the average frequency shifts from the separate moieties to the tetramer spectrum are in agreement with the MP2 calculations, except for the symmetric stretching of HCN, calculated as −4 cm$^{-1}$ (while the corresponding MP2 value is +14 cm$^{-1}$). Our calculated B3LYP average changes are the blue shifts of 74 and 77 cm$^{-1}$ for the bending modes and the red shifts of 93 cm$^{-1}$ for the asymmetric stretching mode of HCN and 15 and 5 cm$^{-1}$ for the symmetric and asymmetric stretching modes, respectively, of $H_2O$.

## 4. Conclusion

Ab initio calculations at the MBPT/MP2 and DFT/B3LYP levels of theory with the 6-311++G(d,p) basis set have been performed for investigating equilibrium structures, vibrational spectra, energetics, and cooperative effects on the properties of mixed HCN−water clusters. Correlation effects and counterpoise correction have been systematically analyzed. High-order electron correlation effects are found to give only a minor contribution to the binding. The contribution beyond fourth-order, as obtained by the difference between MP4 and CCSD(T), decreased the binding energy by 0.16 kJ/mol in $H_2O\cdots HCN\cdots H_2O$, 0.27 kJ/mol in $HCN\cdots HCN$, and 0.34 kJ/mol in $H_2O\cdots HCN$ and $HCN\cdots H_2O$. From CCSD to CCSD(T), the correlation contribution amounted to only 0.60, 0.26, and 0.23

kJ/mol, respectively, in the interaction of these clusters. Counterpoise correction amounts to 2.5 kJ/mol in the binding energies of both the tetramer and $(HCN)_2$.

The B3LYP results for the binding energies of the trimer and tetramer have been larger than those calculated with MP2. The intermolecular distances were also calculated to be shorter with the B3LYP functional. This trend observed in applying DFT/B3LYP for the hydrogen-bonded clusters has also been noted before.[32] Also in this present study, we note that this functional has not described correctly the out-of-plane bend angle, present in the complexes when $H_2O$ acts a proton acceptor. This angle is known in the case of the $H_2O\cdots HCN$ dimer and is correctly described by MP2. By using different correlated methods, we could verify that most of the cooperative effects were already obtained at the MP2 level and that the high-order correlation effects were less important. The electrostatic contribution in the hydrogen-bonded clusters has led to increased dipole moments. For instance, the dipole moments of the trimer and tetramer were larger than the sum of the separate moieties by about 1 D. We have estimated that the cooperativity contribution to the binding energy of the mixed trimer accounts for about 10% of the total interaction energy, which is in agreement with other recent studies.[22] In the case of the mixed tetramer, $H_2O\cdots HCN\cdots HCN\cdots H_2O$, the energy associated with the $HCN\cdots HCN$ hydrogen bonding is ca. 8 kJ/mol larger than that in the corresponding isolated dimer. This cooperative effect is well-described by the MBPT/CC methods, and the large-order electron correlation effects are found to be very small, being well-described by MP2. The cooperative effects are more difficult to be described in the vibrational spectra of the complexes studied here. The calculated intramolecular harmonic frequencies changed little by the presence of the hydrogen bonds. However, we note that all of the $O-H\cdots N$ stretching bands were shifted to lower frequencies. Finally, this study presents a systematic analysis of hydrogen-bonded HCN−water clusters and the effects on structures, binding, infrared spectra, and cooperativity.

**Acknowledgment.** This work was supported by the Brazilian agencies CNPq and FAPESP.

## References and Notes

(1) Heikkilä, A.; Pettersson, M.; Lundell, J.; Khriachtchev, L.; Räsänen, M. *J. Phys. Chem. A* **1999**, *103*, 2945.

(2) Fillery-Travis, A. J.; Legon, A. C.; Willoughby, L. C. *Proc. R. Soc. London, Ser. A* **1984**, *396*, 405.

(3) Gutowski, H. S.; Germann, T. C.; Augspurger, J. D.; Dykstra, C. E. *J. Chem. Phys.* **1992**, *96*, 5808.

(4) Gottlieb, C. A.; Apponi, A. J.; McCarthy, M. C.; Thaddeus, P. *J. Chem Phys.* **2000**, *113*, 1910.

(5) Vigouroux, C.; Fayt, A.; Guarnieri, A.; Huckauf, A.; Bürger, H.; Lentz, D.; Preugschat, D. *J. Mol. Spectrosc.* **2000**, *202*, 1.

(6) Liebman, S. A.; Rodriguez, R. A. P.; Matthews, C. N. *Adv. Space Res.* **1994**, *15*, 71.

(7) Matthews, C. N. *Origins Life Evol. Biosphere* **1992**, *21*, 421.

(8) Meotner, M.; Speller, C. V. *J. Phys. Chem.* **1989**, *93*, 3663.

(9) Rivelino, R.; Canuto, S. *Chem. Phys. Lett.* **2000**, *322*, 207.

(10) Heikkilä, A. T.; Lundell, J. *J. Phys. Chem. A* **2000**, *104*, 6637.

(11) Smith, D. M. A.; Smets, J.; Elkadi, Y.; Adamowicz, L. *Chem. Phys. Lett.* **1998**, *288*, 609.

(12) Tshehla, T. M.; Ford, T. A. *Bull. Pol. Acad. Sci., Chem.* **1994**, *42*, 397.

(13) Turi, L.; Dannenberg, J. J. *J. Phys. Chem.* **1993**, *97*, 7899.

(14) Samuels, A. C.; Jensen, J. O.; Krishnan, P. N.; Burke, L. A. *THEOCHEM* **1998**, *427*, 199.

(15) Cruzan, J. D.; Braly, L. B.; Liu, K.; Brown, M. G.; Loeser, J. G.; Saykally, R. J. *Science* **1996**, *271*, 59.

(16) Xantheas, S. S. *J. Chem Phys.* **1994**, *100*, 7523.

(17) Jeffrey, G. A.; Gress, M. E.; Takagi, S. *J. Am. Chem. Soc.* **1977**, *99*, 609.

(18) Steiner, T.; Mason, S. A.; Saenger, W. *J. Am. Chem. Soc.* **1990**, *112*, 6184.

(19) Jeffrey, G. A.; Saenger, W. *Hydrogen Bonding in Biological Structures*; Springer-Verlag: Berlin, 1991.

(20) For a recent review, see: Scheiner, S. *Hydrogen Bonding: A Theoretical Perspective*; Oxford University Press: New York, 1997.

(21) Masella, M.; Gresh, N.; Flament, J.-P. *J. Chem. Soc., Faraday Trans.* **1998**, *94*, 2745.

(22) Cabaleiro-Lago, E. M.; Ríos, A. *J. Phys. Chem. A* **1999**, *103*, 6468. Cabaleiro-Lago, E. M.; Hermida-Ramón, J. M.; Peña-Gallego, A.; Martínez-Núñez, E.; Fernández-Ramos, A. *THEOCHEM* **2000**, *498*, 21.

(23) Sum, A. K.; Sandler, S. I. *J. Phys. Chem. A* **2000**, *104*, 1121.

(24) Frisch, M. J.; Trucks, G. W.; Schlegel, H. B.; Scuseria, G. E.; Robb, M. A.; Cheeseman, J. R.; Zakrzewski, V. G.; Montgomery, J. A., Jr.; Stratmann, R. E.; Burant, J. C.; Dapprich, S.; Millam, J. M.; Daniels, A. D.; Kudin, K. N.; Strain, M. C.; Farkas, O.; Tomasi, J.; Barone, V.; Cossi, M.; Cammi, R.; Mennucci, B.; Pomelli, C.; Adamo, C.; Clifford, S.; Ochterski, J.; Petersson, G. A.; Ayala, P. Y.; Cui, Q.; Morokuma, K.; Malick, D. K.; Rabuck, A. D.; Raghavachari, K.; Foresman, J. B.; Cioslowski, J.; Ortiz, J. V.; Stefanov, B. B.; Liu, G.; Liashenko, A.; Piskorz, P.; Komaromi, I.; Gomperts, R.; Martin, R. L.; Fox, D. J.; Keith, T.; Al-Laham, M. A.; Peng, C. Y.; Nanayakkara, A.; Gonzalez, C.; Challacombe, M.; Gill, P. M. W.; Johnson, B. G.; Chen, W.; Wong, M. W.; Andres, J. L.; Head-Gordon, M.; Replogle, E. S.; Pople, J. A. *Gaussian 98*, revision A.7; Gaussian, Inc.: Pittsburgh, PA, 1998.

(25) Becke, A. D. *J. Chem. Phys.* **1993**, *98*, 5648.

(26) Lee, C.; Yang, W.; Parr, R. G. *Phys. Rev. B* **1998**, *37*, 785.

(27) Bartlett, R. J. *J. Phys. Chem.* **1989**, *93*, 1697.

(28) Raghavachari, K. *Annu. Rev. Phys. Chem.* **1991**, *42*, 615.

(29) van Duijneveldt, F. B.; van Duijneveldt-van de Rijdt, J. G. C. M.; van Lenthe, J. H. *Chem. Rev.* **1994**, *94*, 1873.

(30) Boys, S. F.; Bernardi, F. *Mol. Phys.* **1970**, *19*, 553.

(31) Chalasinski, G.; Szczesniak, M. M. *Chem. Rev.* **1994**, *94*, 1723.

(32) Del Bene, J. E.; Person, W. B.; Szczepaniac, K. *J. Phys. Chem.* **1995**, *99*, 10705.

(33) Harris, D. C.; Bertolucci, M. D. *Symmetry and Spectroscopy. An Introduction to Vibrational and Electronic Spectroscopy*; Dover: New York, 1989.

(34) Bentwood, R. M.; Barnes, A.; Orville-Thomas, W. *J. Mol. Spectrosc.* **1980**, *84*, 391.